Full Length Research Paper

Nonlinear finite element analysis of reinforced concrete plates modeled by layered composites

Rifat SEZER[1]* and Muhammed D. TEKIN[2]

[1]Department of Civil Engineering, Engineering and Architecture Faculty, Selcuk University, Konya, Turkey.
[2]Department of Civil Engineering, Celal Bayar University, Manisa, Turkey.

In this study, finite elements method (FEM) was used for the nonlinear analysis of reinforced concrete (R/C) plates under incremental loading up to failure load. Layered composite material model (LCMM) was used for the modeling of reinforced concrete plates. This approach differs from the other approaches since it considers the effect of tensile stiffness of concrete between cracks and uses a criterion based on the fracture energy concept considering the effect of finite element mesh size. Load-displacement relationships were determined according to the 'layered composite material approach'. The results of the analyses were compared and found to be in agreement with the experimental results and the results of past studies. A computer program prepared with Fortran PowerStation 4.0 programming language was used in this study.

Key words: Non-linear plate analysis**,** finite elements method, layered composite materials.

INTRODUCTION

The analysis of reinforced concrete structures using an analytical method is an advanced but complex process due to the following reasons: 1) Reinforced concrete structures are formed by the combination of two different materials that is concrete and steel, 2) the behavior due to tensile crack, biaxial rigidity, nonlinear stress-strain relationship of concrete and strain softening, 3) reinforcement slip and aggregate interlock, etc. In general, for the analysis of reinforced concrete plates and beams by FEM, two different approaches are used: a) modified stiffness approach, b) layered approach (is also used in this study). Some of the important studies carried out in the past for the nonlinear analysis of reinforced concrete plates are the following: Kupfer et al. (1969) examined the behavior of concrete under biaxial tensile stress experimentally. Jofriet et al. (1971) studied the finite elements method to determine the crack effect of concrete on the nonlinear analysis of reinforced concrete slabs. Hand et al. (1973) investigated the nonlinear analysis of the layered models of reinforced concrete

plates and shells. Jones (1975) described the mechanical modeling of the composite materials having layers of different characteristics. Lin and Scordelis (1975) researched the nonlinear analysis of reinforced concrete shells and plates of general form. Bashur and Darwin (1978) performed the nonlinear modeling of reinforced concrete plates using finite elements method. Gilbert and Warner (1978) analyzed the effect of tensile stiffness on reinforced concrete slabs. Bathe (1982) explained the nonlinear analysis of plates and shells in detail according to the finite elements method. Bazant and Oh (1983) studied the crack band model on the fracture mechanics of concrete. Choi and Kwak (1990) investigated the effect of finite element mesh dimension on the nonlinear analysis of reinforced concrete structures. Hu and Schnobrich (1991) carried out the nonlinear analysis of reinforced concrete plates and shells under gradually increasing loads by the aid of finite elements method.

Sathurappan et al. (1992) studied the nonlinear analysis of the reinforced and prestressed concrete plates and shells by using the finite elements method. Sezer (1995) investigated the nonlinear analysis of reinforced concrete plates according to the finite elements method. Özer (2006) described the nonlinear analysis of structural systems in detail according to

_____

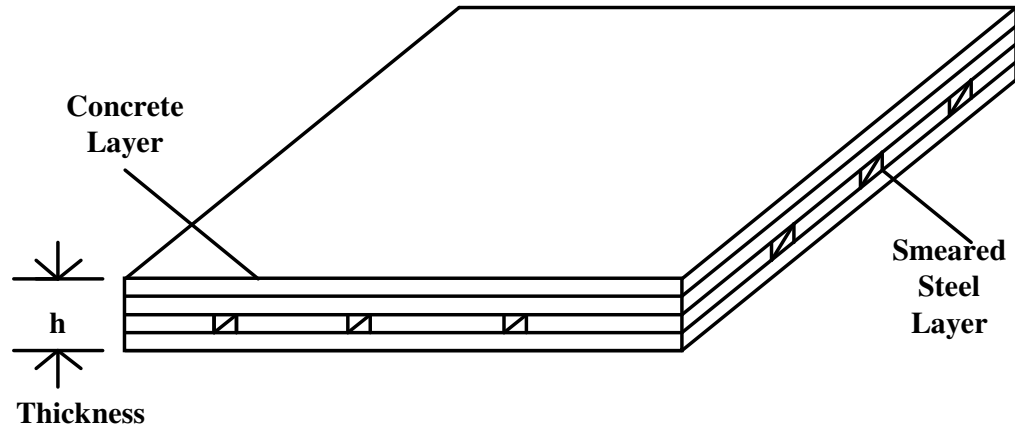*Corresponding author. E-mail: rsezer@selcuk.edu.tr. Tel: +90 332 2232160. Fax: +90 332 2410635.
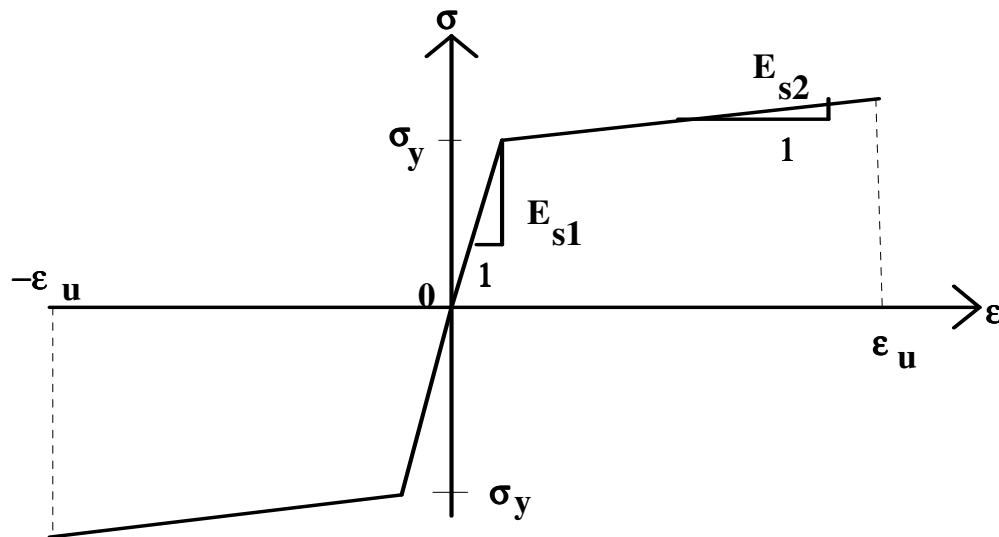
Figure 1. Layered system.

Figure 2. Idealized uniaxial stress-strain relationship of steel.

various methods. Zhang et al. (2007) performed the nonlinear analysis of the reinforced concrete cylindrical shells and plates modeled with layered rectangular elements by using finite elements method.

MATERIAL PROPERTIES AND ASSUMPTIONS

In order to formulize the basic relationships of a reinforced concrete member of a layer, the following simplified assumptions were made: a) concrete and embedded steel reinforcement are divided into some imaginary layers (Figure 1); b) the bending of plates occurs according to the Mindlin plate theory, c) steel reinforcement resists only uniaxial stresses, and d) there is perfect bond between steel and concrete (Choi and Kwak, 1990).

Steel

Reinforcing steel with σ_y yield stress was assumed to be a material with linear strain hardening (Figure 2). Stress-strain relationship of the steel can be expressed as in the following with reference to local axes oriented both parallel and perpendicular to the direction of the reinforcement.

$$\begin{Bmatrix} \sigma_1 \\ \sigma_2 \\ \tau_{12} \end{Bmatrix} = \begin{bmatrix} E_{s1} & 0 & 0 \\ 0 & 0 & 0 \\ 0 & 0 & 0 \end{bmatrix} \begin{Bmatrix} \varepsilon_1 \\ \varepsilon_2 \\ \gamma_{12} \end{Bmatrix} \tag{1}$$
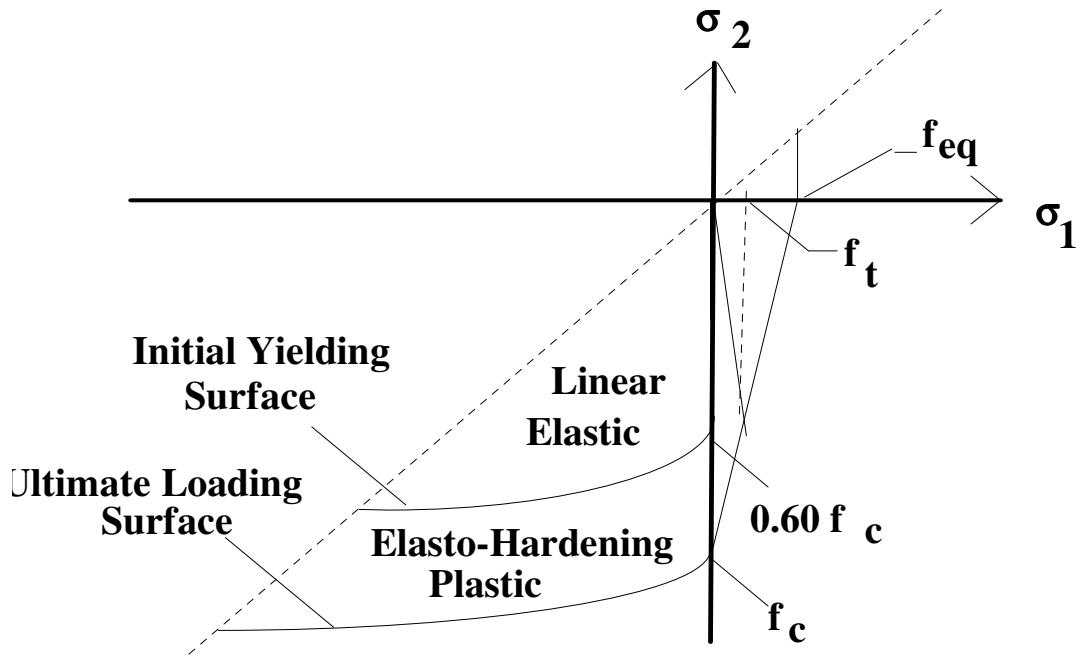
Here, E_{s1} is the first modulus of elasticity of steel. When

Figure 3. Biaxial strength envelops of concrete.

Concrete

Concrete under biaxial stress was assumed to behave linearly elastic at the tension zone. As seen in Figure 3, f_{eq} is the end-point stress on the right. In this case the stress linearly decreases by equal amount increase in the uniaxial strain. If concrete is at the compression zone, it will be accepted as elasto-plastic hardening model. Similarly, a yielding criterion was defined in Equation 2 by Kupfer et al. (1969).

$$F = [(\sigma_1 + \sigma_2)^2/(\sigma_2 + 3.65\sigma_1)] - Af_c = 0 \qquad (2)$$

Here, σ_1 and σ_2 are the principal stresses; f_c represents the uniaxial compression strength and A is the parameter symbolizing plastic yielding from initial yielding surface (A = 0.6) to final loading surface (A = 1.0) (Kupfer et al., 1969). In order to check the cracking condition of concrete continuously, similar to the yielding surface of Equation 2, a crack surface (Figure 4) was determined using strain terms and defined by the following equation:

$$C = [(\varepsilon_1 + \varepsilon_2)^2/(\varepsilon_2 + 3.65\varepsilon_1)] - \varepsilon_{cu} = 0 \qquad (3)$$

Here, ε_1 and ε_2 are the principal strains, and ε_{cu} is the maximum strain of concrete under compression (Choi and Kwak, 1990).

Cracked stiffness of concrete

When principal tensile strain is exceeded ε_0 (Figure 5), cracks will develop in a direction perpendicular to the principal stress. Shear modulus should be reduced by cracking. However, intending to determine an effective shear modulus is more complex besides determining the lever effect and aggregate locking effects. Therefore, the value of cracked shear modulus was assumed to be continuously constant also after the cracking event; that is in Equation 4 $\lambda = 0.4$. Then the cracked stiffness will be accepted as the following:

$$\begin{Bmatrix} \sigma_1 \\ \sigma_2 \\ \tau_{12} \end{Bmatrix} = \frac{1}{1-\nu^2} \begin{bmatrix} E_1 & 0 & 0 \\ 0 & 0 & 0 \\ 0 & 0 & \lambda\frac{1-\nu}{2}G \end{bmatrix} \begin{Bmatrix} \varepsilon_1 \\ \varepsilon_2 \\ \gamma_{12} \end{Bmatrix} \qquad (4)$$

Here, axes 1 and 2 are respectively parallel and perpendicular to the cracks. G and λ are the shear modulus of uncracked concrete and shear constant of the cracked concrete, respectively. If the cracking of concrete occurs biaxially, then E_1 will be taken as zero (Choi and Kwak, 1990; Hu and Schnobrich, 1991).

TENSION STIFFENING EFFECT

The increase in tensile stiffness of concrete can be provided by using the stress-strain relationship of the decreasing section at the tensile zone (Lin and Scordelis,
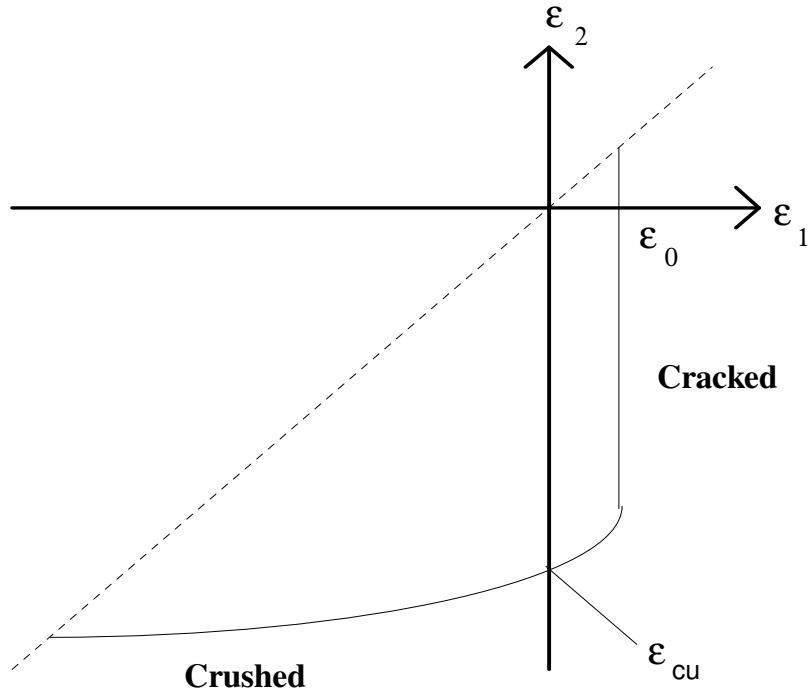
steel yields the second modulus of elasticity E_{s2} is used in place of E_{s1} (Choi and Kwak, 1990).
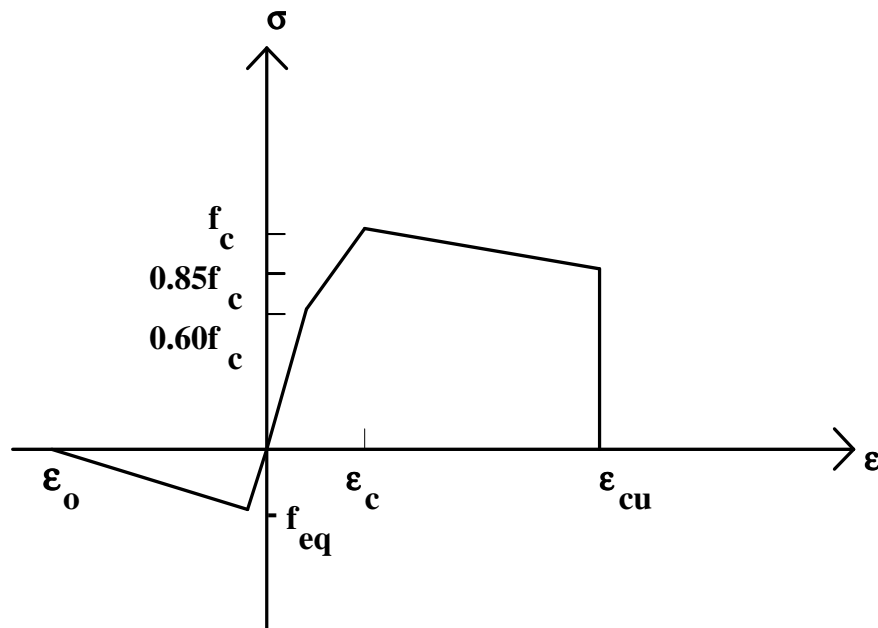
Figure 4. Failure surface of concrete.

Figure 5. Idealized uniaxial stress-strain relationship of concrete.

1975; Gilbert and Warner, 1978). On the other hand, the nonlinear form of the cracking model should be used in order to estimate the displacements of the structure more precisely. About this subject, stress-controlled cracking model was firstly used by Rashid (Choi and Kwak, 1990) for the numerical analysis of the reinforced concrete structures. However, this model has some negative sides such as being independent from finite element network dimensions, etc. Many researchers most of which were interested in cracking mechanics suggested the "cracked band theory", the simplest model of fictive cracking models on planar concrete panels. Two basic
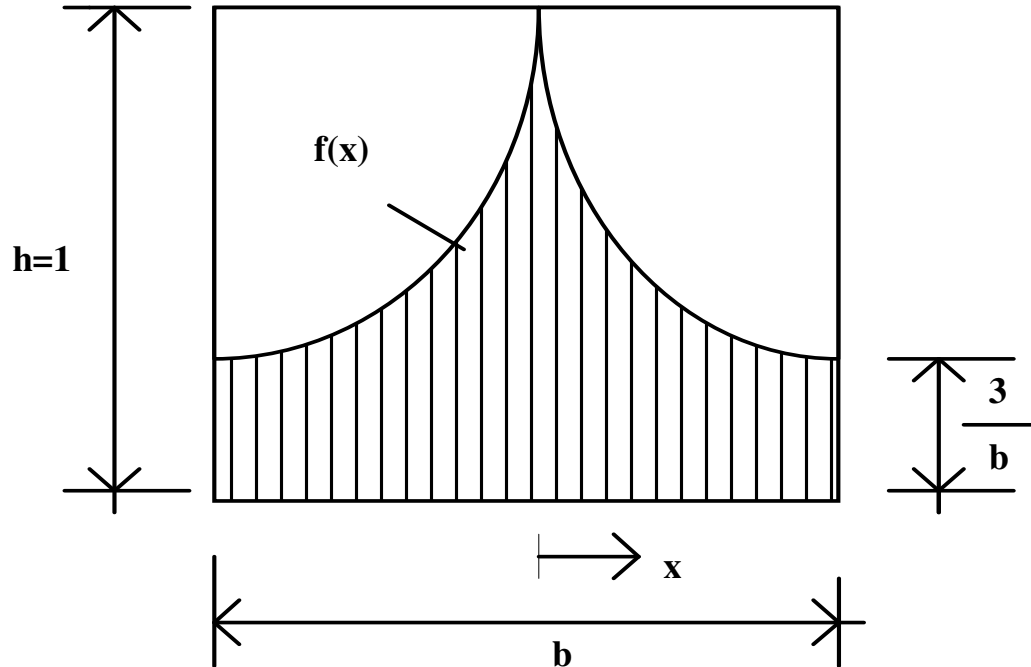
Figure 6. Assumed distribution of microcracks in an element.

assumptions of this model are: a) the deformation inside the band is uniform; b) the width of the cracking zone has a certain b value directly proportional to three times of the maximum aggregate size (3 x 25.4 mm). Then, the equation for finding ε_0 is given in the following:

$$\varepsilon_0 = \frac{2G_f}{f_t b} \qquad (5)$$

This model can be successfully applied to the reinforced concrete problems, when relatively small finite element network dimension is used. However, Equation 5 will not be sufficient for the direct application of this model to the numerical analysis of reinforced concrete structures modeled with relatively large finite element network dimensions (Bazant and Oh, 1983; Choi and Kwak, 1990).

APPLIED CRACK MODEL

A new criterion applicable to an extremely large finite element network dimension was used for the nonlinear analysis of the reinforced concrete structures.

Microcrack distributions

At first, in order to formulize the distribution of the microcracks of a member, an exponential function is given in the following (Figure 6):

$$f(x) = \alpha \, e^{\beta x} \qquad (6)$$

Here, α and β are specifiable constants. If the boundary conditions, that is $f(0) = 1.0$ and $f(b/2) = 3/b$ are substituted in Equation 6, the following equation will be determined.

$$f(x) = e^{-2b \ln (b/3) \, x} \qquad (7)$$

Here, b is the width of the member. For the expressions of $f(x)$ function defined in Equations 6 and 7: 1) the distribution of microcracks has a symmetrical characteristic as shown in Figure 6; 2) the typical dimension of microcrack at the end of the finite member network is 3/b. The second property proves that the microcrack distribution is uniform for the condition of a width less than 76 mm (Bazant and Oh, 1983; Choi and Kwak, 1990).

Fracture energy

The stress-strain relationship and cracking energy of concrete are given in the following:

$$G_f = \frac{1}{2} \varepsilon_0 f_t \int_0^{b/2} f(x) dx 2 \qquad (8)$$

Here, f_t is the tensile strength of concrete, ε_0 is the strain
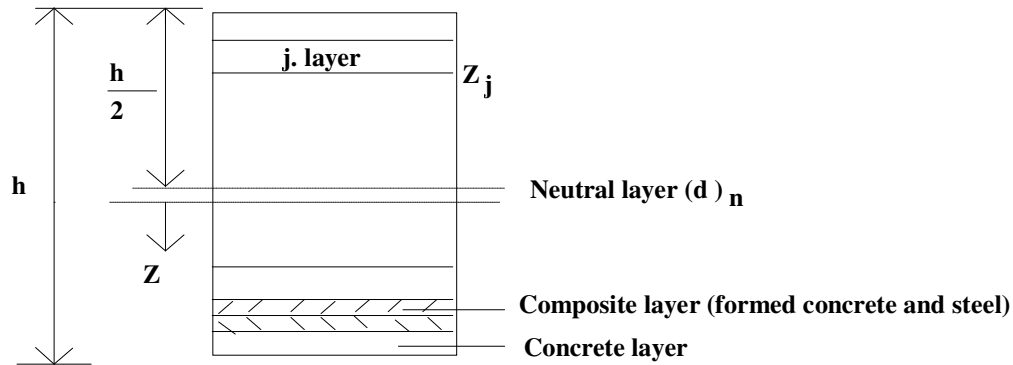
Figure 7. A layered section.

at the end of the decreasing strain zone and G_f is the consumed cracking energy of a crack with unit length through the unit thickness. If G_f and f_t are known from measurements, then ε_o can be calculated as the following:

$$\varepsilon_0 = \frac{G_f}{f_t \int_0^{b/2} f(x)dx} \tag{9}$$

If finite element network dimension is changed, E_o can be calculated by using Equation 7. For $f(x) = 1.0$, the suggested criterion in Equations 5 and 9 gives the same result, that is finite element network dimension is equal to or less than 76 mm. When finite element network dimension is greater than 76 mm, the microcracks distribution of the member should be accepted according to the $f(x)$ function in Equation 7 as applied in most of the practical conditions.

REINFORCED CONCRETE APPLICATION OF FINITE ELEMENT METHOD

As shown in Figure 7, a typical finite element is divided into imaginary concrete and composite (formed with concrete and steel) layers. It is assumed that the displacement area of the member is continuous and there are no gaps between layers. The material properties of each layer may differ but they present a homogeneous structure through the thickness of the layer. Then, the integration volume involving the material properties can be written as the following:

$$\int [B]^T [D][B]dv = \sum_{i=1}^{n_k} \int_v [B]^T [D_k]_i [B]dV + \sum_{j=1}^{n_c} \int_v [B]^T [D_c]_j [B]dV \tag{10}$$

Here, $[D_k]_i$ and $[D_c]_i$ are the material matrices of the ith

composite layer and jth concrete layer, and n_k and n_c are the number of composite and concrete layers respectively. The displacement area based on Mindlin hypothesis can be defined in matrix form as in the following:

$$\{d\} = \begin{Bmatrix} w \\ \theta_x \\ \theta_y \end{Bmatrix} = \sum_{j=1}^{n} \begin{bmatrix} N_j & 0 & 0 \\ 0 & N_j & 0 \\ 0 & 0 & N_j \end{bmatrix} \begin{Bmatrix} w \\ \theta_x \\ \theta_y \end{Bmatrix}_j \tag{11}$$

Where n is the number of nodes and N_j is the interpolation function. The relationship between strain and displacements can be written as:

$$\begin{Bmatrix} \varepsilon_x \\ \varepsilon_y \\ \gamma xy \end{Bmatrix} = \begin{bmatrix} 0 & -\dfrac{\partial N}{\partial x} & 0 \\ 0 & 0 & -\dfrac{\partial N}{\partial y} \\ 0 & -\dfrac{\partial N}{\partial x} & -\dfrac{\partial N}{\partial y} \end{bmatrix} \begin{Bmatrix} w \\ \theta_x \\ \theta_y \end{Bmatrix} \tag{12}$$

Or

$$\{\varepsilon_p\} = [B_p]\{u\} \tag{13}$$

The relationship between transversal shear strains and displacements can be given as:

$$\begin{Bmatrix} \gamma_{xz} \\ \gamma_{yz} \end{Bmatrix} = \begin{bmatrix} -\dfrac{\partial N}{\partial y} & -N & 0 \\ -\dfrac{\partial N}{\partial y} & 0 & -N \end{bmatrix} \begin{Bmatrix} w \\ \theta_x \\ \theta_y \end{Bmatrix} \tag{14}$$

Or

$$\{\varepsilon_t\} = [B_t]\{u\} \tag{15}$$

After substituting the sub-equations of Equations 13 and

15 into Equation 10, and rearranging the material matrix, the member stiffness matrix can be written as the following:

$$[K] = \int_v [B_p]^T [D_p][B_p] \, dV + \int_v [B_t]^T [D_t][B_t] \, dV \qquad (16)$$

Here, $[D_p]$ and $[D_t]$ given in Equation 17 are the flexural and shear sections of the material matrix, respectively (Choi and Kwak, 1990):

$$D_{pij} = \sum_{k=1}^{N} (Q^-_{ij})_k (h_k z_k + \frac{h^3_k}{12}),$$

$$[D_t] = \frac{Ehk}{2(1+v)}\begin{bmatrix} 1 & 0 \\ 0 & 1 \end{bmatrix} \qquad (17)$$

Where z_k is the height from the central surface to the center of the kth layer, h_k is the thickness of the layer, Q^-_{ij} represents the flexural rigidities of the kth layer which can be calculated by Equation 18 for the orthotropic plates. k (in the second equation) is the shear correction factor having the value of 5/6, E is the modulus of elasticity and v is the Poisson's ratio:

$$\left(Q^-_{11}\right)_k = \frac{E^k_1}{1 - v^k_{12} v^k_{21}} \quad , \quad \left(Q^-_{12}\right)_k = \frac{v^k_{12} E^k_1}{1 - v^k_{12} v^k_{21}} ,$$

$$\left(Q^-_{22}\right)_k = \frac{E^k_2}{1 - v^k_{12} v^k_{21}} \qquad (18)$$

$$\left(Q^-_{16}\right)_k = 0 \ , \ \left(Q^-_{26}\right)_k = 0 \ , \ \left(Q^-_{66}\right)_k = G^k_{12} \qquad (19)$$

Here, G^k_{12} is the shear modulus parallel to surface 1. The calculation procedure of node displacement parameters and each layer's strain members determined by Equations 13 and 15 are given in the following for both concrete and composite layers (Jones, 1975; Bathe, 1982).

$$\{\varepsilon_c\}_j = \begin{cases} \varepsilon_{xj} = (-d_{nx} + 0.5h + z_j)\frac{\partial\theta_x}{\partial x} \\ \varepsilon_{yj} = (-d_{ny} + 0.5h + z_j)\frac{\partial\theta_y}{\partial y} \\ \gamma_{xyj} = (-d_{nxy} + 0.5h + z_j)\left(\frac{\partial\theta_x}{\partial x} + \frac{\partial\theta_y}{\partial y}\right) \\ \gamma_{xzj} = \frac{\partial w}{\partial x} - \theta_x \\ \gamma_{xzj} = \frac{\partial w}{\partial x} - \theta_x \end{cases},$$

$$\{\varepsilon_s\}_i = \begin{cases} \varepsilon_{xi} = (d_x - d_{nx})\frac{\partial\theta x}{\partial x} \\ \varepsilon_{yi} = (d_y - d_{ny})\frac{\partial\theta y}{\partial y} \end{cases} \qquad (20)$$

Here, d_{nx}, d_{ny} and d_{nxy} given to prevent the development of unwanted forces on the plane represent the neutral

axis depths (Figure 7) that can be calculated under the condition of $\int\sigma_x \, dz = \int\sigma_y \, dz = \int\tau_{xy} \, dz = 0$; where z is the depth measured from the central surface (Figure 7). Additionally, the simplified assumptions used here are: 1) Shear modulus G is constant through the depth, 2) d_{nxy} value is nearly equal to h/2 where h is the thickness of the member, 3) d_x and d_y are the useful heights in x and y directions, 4) z_j is the height measured from the central surface to the center of the concrete layer (Figure 7).

$$\{\sigma_c\}_i = [Q^-]_{ki}\{\varepsilon_c\}_i \qquad (21)$$

Or

$$\begin{Bmatrix} \sigma_x \\ \sigma_y \\ \tau_{xy} \end{Bmatrix}_{cj} = \begin{bmatrix} Q^-_{11} & Q^-_{12} & 0 \\ Q^-_{12} & Q^-_{22} & 0 \\ 0 & 0 & Q^-_{66} \end{bmatrix}\begin{Bmatrix} \varepsilon_x \\ \varepsilon_y \\ \gamma_{xy} \end{Bmatrix}_{cj} \qquad (22)$$

The stress-strain relationship in the local axes parallel and perpendicular to the reinforcement bar can be written as Equation 23 by using Equation 1.

$$\{\sigma_s\}_i = [Q^-]_{ki}\{\varepsilon_s\}_i \qquad (23)$$

Here, $\{\sigma_s\}_i$ ve $\{\varepsilon_s\}_i$ represent the stress and strain values at the center of the ith steel layer and $\{\sigma_c\}_j$ and $\{\varepsilon_c\}_j$ represent the stress and strain values at the center of the jth concrete layer, respectively (Jones, 1975; Choi and Kwak, 1990). In nonlinear problems, the calculated stresses do not agree with the real stresses due to unbalanced node forces. The equivalent node forces can be determined statically in the equivalent stress zone by Equation 24.

$$\{R\}_{equivalent} = \int_v [B]^T \{\sigma\}dV = \int_v [B]^T \{\sigma_p\}dV + \int_v [B]^T \{\sigma_t\}dV \qquad (24)$$

Unbalanced node forces can be calculated by using Equation 25.

$$\{R\}_{unbalanced} = \{R\}_{applied} = \{R\}_{equivalent} \qquad (25)$$

In the solution, a load increase was applied to determine the unbalanced node forces that were iteratively recalculated to approach the convergence tolerance.

NUMERICAL EXAMPLE

A two-way slab supported by its four edges (Figure 8) and solved in the literature was resolved by the aid of the newly developed computer program. The slab subjected
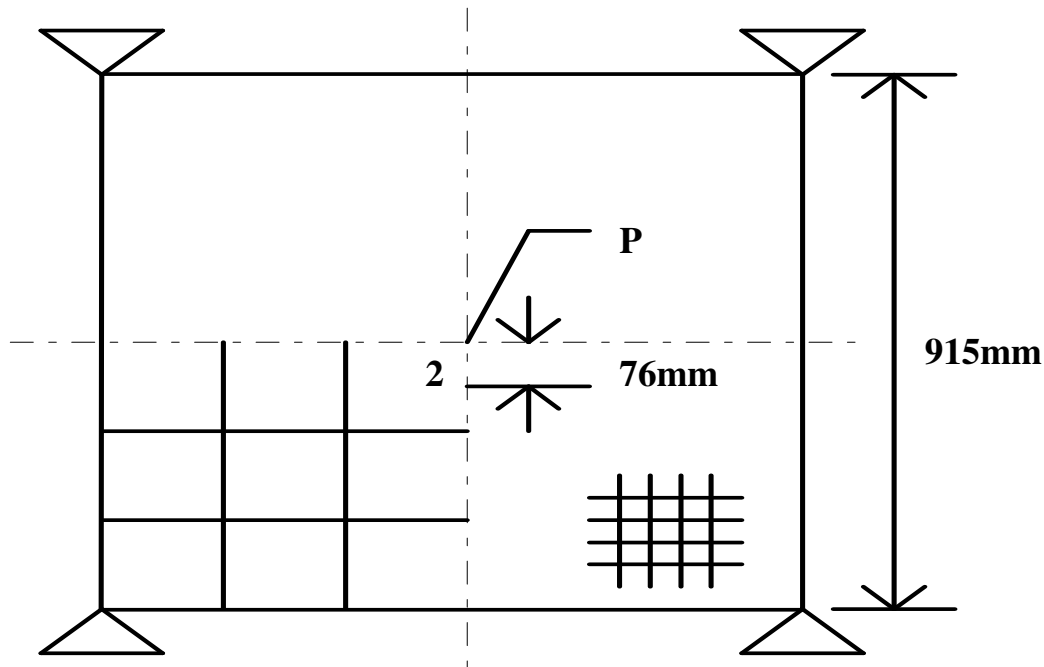
Figure 8. Corner-supported two-way slab.

Table 1. Load-displacement values at node 2 in Figure 8.

		Displacement (mm)						
Laod No	Load (kN)	Experiment	Choi	Bashur	This study	Jofriet	Hand	Lin
1	2.7	0.25	0.48	0.48	0.47	0.48	0.48	0.48
2	5.4	0.83	0.83	0.83	0.93	0.83	0.83	0.83
3	8.1	2.33	2.25	2.00	1.69	1.83	2.83	1.33
4	10.8	4.70	4.70	4.33	4.74	4.00	5.10	4.33
5	13.5	7.54	7.52	7.54	7.30	7.00	-	-

to a single load at the center has a square shape with 915 mm side length, 44.5 mm thickness and the ratio of reinforcement in isotropic network shape is 0.0085. The selected material properties are: concrete's Poisson's ratio ν_c = 0.167, tensile strength f_{ctk} = 2.15 N/mm^2, compression strength f_{ck} = 38 N/mm^2, modulus of elasticity E_c = 3.10^4 N/mm^2, cracking energy G_f = 0.09 N/mm and the number of concrete layers is n_c = 8. The yield strength and modulus of elasticity of steel are respectively f_{yk} = 276 N/mm^2 and E_s = 3.10^4 N/mm^2. The useful height is d = 33.3 mm (Choi and Kwak, 1990). The finite element network used in this study is given in Figure 8. The displacement amounts at node 2 with respect to load increases were determined in agreement with the results of literature. The load-displacement values are given in Table 1. The graphical representation of load-displacement relationship at node 2 is given in Figure 9. The displacement at node 2 can be approximately calculated by making interpolation with the displacements of the adjacent nodes.

CONCLUSION

In this study, isoparametric members with four, eight and nine nodes were used to perform the finite element modeling by using Layered Approach. The reinforced concrete plate (Figure 8) supported by its four edges was solved with a newly developed finite element model program prepared with Fortran PowerStation 4.0 computer programming language. The results are compared with the results of literature for the same plate in Table 2. After comparing the results of this study with the results of literature and experimental study for the same subject, the results of this study were in agreement with the results of both literature and experimental study.
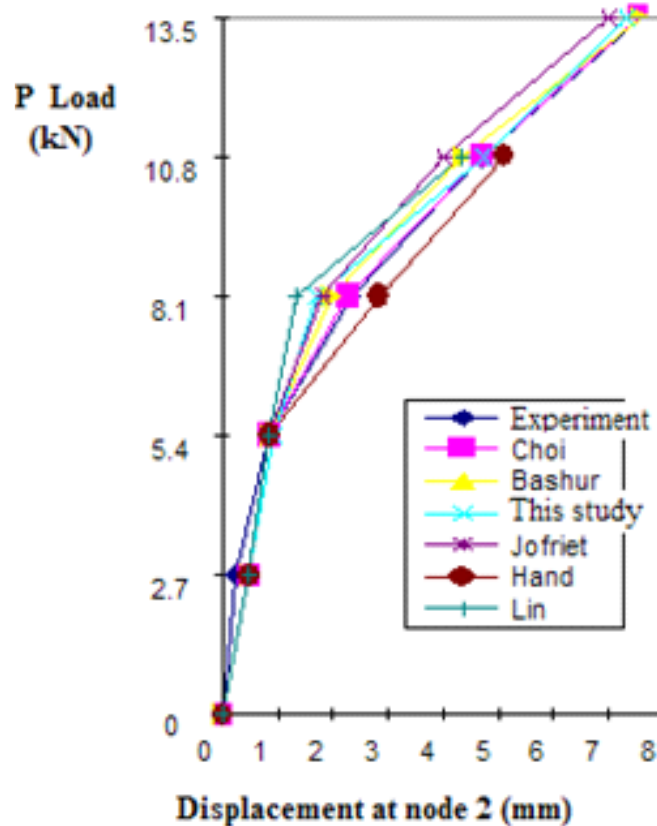
Figure 9. Load-displacement relationship at node 2.

Table 2. The comparison of test results determined by this study with the test results of literature (for the plate in Figure 8).

Average differences according to the test results of literature (%)					
Choi	Bashur	This study	Hand	Jofriet	Lin
10.2	14.0	17.8	18.2	18.5	24.8

REFERENCES

Bashur FK, Darwin D (1978). Nonlinear model for reinforced concrete slabs. J. Struct. Div., ASCE, 104: 157-170.

Bathe KJ (1982). Finite element procedures in engineering analysis. Prentice –Hall Inc., New Jersey, 371-378.

Bazant ZP, Oh BH (1983). Crack band theory for fracture of concrete. Mater. Struct., 16: 155-176.

Choi CK, Kwak HG (1990). The effect of finite element mesh size in nonlinear analysis of reinforced concrete structures. Comput. Struct., 36(5): 807-815.

Gilbert RI, Warner RF (1978). Tension stiffening in reinforced concrete slabs. J. Struct. Div. ASCE, 104: 1885-1900.

Hand FR, Pecknold DA, Schnobrich WC (1973). Nonlinear layered analysis of RC plates and shells. J. Struct. Div. ASCE, 99: 1491-1505.

Hu HT, Schnobrich WC (1991). Nonlinear finite element analysis of reinforced concrete plates and shells under monotonic loading. Comput. Struct., 38(5/6): 637-651.

Jofriet JC, McNeice GM (1971). Finite element analysis of RS slabs. J. Struct. Div. ASCE, 97: 785-806.

Jones RM (1975). Mechanics of composite materials. Mc Graw-Hill. pp. 147-173.

Kupfer H, Hilsolort HK, Rush H (1969). Behavior of concrete under biaxial stresses. J. Am. Coner. Inst., 66: 656-666.

Lin CS, Scordelis AC (1975). Nonlinear analysis of RC shells of General form. J. Struct. Div. ASCE, 101: 523-538.

Özer E (2006). Nonlinear Analysis of Structures Systems. Technical University. Doctorate Lessons Notest. Istanbul. Turkey.

Sathurappan G, Rajagopalan N, Krishnamorthy (1992). Nonlinear finite element analysis of and prestressed concrete slabs with reinforcement (inclusive of prestresing steel) modeled as discrete integral components. Comput. Struct., 44(3): 575-584.

Sezer R (1995). Nonlinear analysis of reinforced concrete plates by finite elements methods. Selcuk University. Graduate School of Natural and Applied Sciences. PhD. Konya. Turkey.

Zhang YX, Bradford MA, Gilbert RI (2007). A layered cylindrical quadrilateral shell element for nonlinear analysis of RC plates structures. Adv. Engineer. Software, 38: 488-500.